

## Investigation of the Influence of UV Radiation on Compositions of Polylactide with Graphite Nanoplatelets

M. M. Gasymov<sup>a</sup>, S. Z. Rogovina<sup>a, \*</sup>, O. P. Kuznetsova<sup>a</sup>, E. O. Perepelitsyna<sup>b</sup>, V. G. Shevchenko<sup>c</sup>, S. M. Lomakin<sup>a, d</sup>, and A. A. Berlin<sup>a</sup>

<sup>a</sup> *Semenov Federal Research Center for Chemical Physics, Russian Academy of Sciences, Moscow, Russia*

<sup>b</sup> *Federal Research Center of Problems of Chemical Physics and Medicinal Chemistry, Russian Academy of Sciences, Chernogolovka, Russia*

<sup>c</sup> *Enikolopov Institute of Synthetic Polymer Materials, Russian Academy of Sciences, Moscow, Russia*

<sup>d</sup> *Emanuel Institute of Biochemical Physics, Russian Academy of Sciences, Moscow, Russia*

\*e-mail: S.Rogovina@mail.ru

Received May 17, 2023; revised October 11, 2023; accepted October 20, 2023

**Abstract**—Composites of polyether polylactide (PLA) synthesized from natural raw materials with graphite nanoplatelets (GNPs), which represent a new type of composite materials based on biodegradable polymers, are obtained by the solid-phase method under the action of shear deformations. The porosity of the composites is evaluated and their electrical and mechanical properties are studied. The effect of UV radiation on the molecular weight and molecular weight distribution of PLA in PLA–GNP composites of different compositions is investigated using the method of exclusion chromatography, and the effect of GNP nanofiller content on the change of their mechanical characteristics in the process of radiation is shown.

**Keywords:** polylactide, graphite nanoplatelets, UV radiation, exclusion chromatography, electrical and mechanical properties

**DOI:** 10.1134/S1990793124020088

### 1. INTRODUCTION

Polymer composites containing various nanosized carbon derivatives as fillers, in particular, two-dimensional layered graphite nanoplatelets (GNPs), are currently attracting the attention of a large number of researchers, since the composites obtained using them have improved strength and thermal characteristics and are a highly sought type of modern material intended for widespread use in various fields [1, 2].

At the same time, thermoplastic biodegradable polyester polylactide (PLA) is one of the most promising so-called green polymers [3, 4]. Synthesized from lactic acid formed during the fermentation of agricultural waste, PLA is close in its mechanical and thermal characteristics to synthetic polymers [5], as a result of which the development of polymer composites based on it is a promising area of research carried out in the field of creating new materials capable of biodegradation.

One of the possible ways to modify PLA, leading to the creation of polymer materials with a wide range of new properties, is to obtain PLA composites using various graphene derivatives as fillers. The structural features and good mechanical characteristics of such carbon compounds make it possible to use them for the

production of various materials based on PLA that have the characteristics required for a specific application [6, 7].

Previously, we conducted a comparative study of the structure and properties of PLA composites with reduced graphene oxide (rGO), obtained by liquid-phase and environmentally friendly solid-phase methods [8], where it was shown that the production method affects the complex of properties and structure of the resulting composites. In particular, it was found that composites obtained by solid-phase mixing under conditions of shear deformation have higher strength characteristics, and their electrical conductivity is more than an order of magnitude higher than the conductivity of composites obtained in the liquid phase. The sharp drop in PLA crystallinity observed in this case is related both to the amorphization of the polymer under the influence of shear deformations and the decrease in the segmental mobility of polymer chains in the presence of nonaggregated filler particles.

At the same time, for PLA–GNP composites synthesized in the liquid phase in chloroform, together with an increase in crystallinity and thermal stability, the formation of a microporous structure was discovered [9].

It is well known that during operation in air, polymer materials are exposed to ultraviolet (UV) irradiation

tion, leading to the destruction of polymer chains and, as a consequence, the destruction of products obtained from them [10]. At the same time, the introduction of different kinds of inorganic fillers can influence this process in different ways, in particular, by eliminating the negative effects of radiation [11].

To assess the influence of UV radiation on the characteristics of polymer materials, physicochemical methods of analysis are usually used such as exclusion chromatography, which allows evaluating changes in the molecular weight and molecular mass characteristics of polymers, together with spectral methods for determining the structure of the polymers formed during degradation (IR spectroscopy, NMR) [12]. Since the degradation of polymers is usually accompanied by a decrease in strength, measuring mechanical parameters makes it possible to determine the effect of radiation on the areas of practical use of such materials.

Studying the resistance of PLA–GNP composites to UV radiation will help expand the possible areas of application of this graphene derivative.

In this paper, the influence of UV irradiation on PLA–GNP composites was studied based on the EC data, and we also measured the mechanical characteristics of the original and irradiated samples.

## 2. EXPERIMENTAL

Polylactide of the PLA 4043D brand (Nature Works, United States ( $M_w = 1.3 \times 10^5$  g/mol,  $T_{\text{melt}} = 155^\circ\text{C}$ )) GNPs produced by XG Sciences (United States), (diameter ( $d$ ) = 10 nm, length ( $L$ ) = 5  $\mu\text{m}$ , ratio  $L/d = 500$ , density  $\rho \leq 1.8$  g/cm<sup>3</sup>) were used in this study.

PLA–GNP composites containing from 0.05 to 5 wt % filler were obtained by the solid-phase method under the action of shear deformations in a closed-type mixer Plastograph EC (Brabender, Germany) at a temperature of 170°C and a rotor speed of 100 rpm [13]. For subsequent studies, films with a thickness of 0.3 mm were pressed on a Carver laboratory press at a temperature of 170°C and a pressure of 10 MPa.

The dielectric properties of composites (dielectric constant, losses, electrical modulus, and conductivity) were studied in the frequency range  $10^{-1}$  to  $10^6$  Hz using a Alpha-A impedance analyzer (Novocontrol Technologies, Netherlands) and a ZGS Alpha Active Sample Cell with gold-plated disk electrodes with a diameter of 20 mm.

The pore sizes were studied using X-ray microtomography, which makes it possible to study the internal volume of an object without destroying the sample. This method is distinguished by the speed of measurements together with the high information content of the data obtained and by the minimization of the influence of the human factor on the research results [14].

The samples were scanned using a Bruker SkyScan 1172 X-ray microtomograph (Bruker micro CT, Belgium). The scanning time was 3 hours. As a result of scanning, a set of shadow projections of the samples was obtained.

The morphometric analysis and porosity calculation were carried out using the CTAN program. In the binary image mode (images with binary grayscale pattern on the display), white corresponds to areas with brightness within the binary threshold (solid) and black corresponds to areas outside this range (void). To correctly display voids and areas of high density, the optimal range of values in the histogram of the brightness distribution was selected (25–255 shades of gray).

Mechanical tests of the resulting composites were carried out on an Instron-3365 tensile testing machine (UK) in the uniaxial tension mode at a constant speed of movement of the upper crosshead of 5.0 mm/min at room temperature. The elastic ( $E$ ) modulus, tensile strength ( $\sigma_R$ ), and elongation at break ( $\epsilon_p$ ) were determined from the tensile stress-elongation ( $\sigma$ – $\epsilon$ ) diagrams. The results were averaged over six to seven samples; the measurement error did not exceed 10% [15].

The influence of exposure to (UV) radiation on the properties of PLA and PLA–GNP films of various composites was studied at a wavelength of 253.7 nm, using four Philips TUV lamps with a power of 11 W, at different exposure times [16].

The molecular mass characteristics of the samples were determined by size EC (gel permeation chromatography (GPC)) on a liquid chromatograph (Waters, United States) equipped with refractometric and UV detectors.

The eluent was tetrahydrofuran (THF), the elution rate was 1 mL/min, the column temperature was 35°C, and the refractometer temperature was 45°C. Polymer samples were dissolved in THF, and the solution was filtered through a 0.2  $\mu\text{m}$  Anotop25 (Whatman, UK) PTFE filter. Two PL-gel 5  $\mu\text{m}$  MIXED-C columns (Agilent, USA) connected in series were used for measurements. The average molecular weight of the polymers was calculated using a calibration curve obtained using polystyrene standards with the MW ranging from 589 to  $3.7 \times 10^6$  Da, Empower software [17].

## 3. RESULTS AND DISCUSSION

A distinctive feature of composite materials containing nanocarbon fillers is their ability to conduct electric current. In relation to this, the dielectric properties of PLA–GNP composites with filler concentrations of 0.1, 0.25, 1, and 5 wt % were studied in this paper. Figure 1 shows the dependence of the dielectric constant  $\epsilon'$  on frequency. At low filler concentrations (less than 1 wt %),  $\epsilon'$  does not depend on frequency and increases slightly as the degree of filling increases. At a filler concentration of 5 wt %,  $\epsilon'$  is largely determined by interfacial polarization caused by the forma-

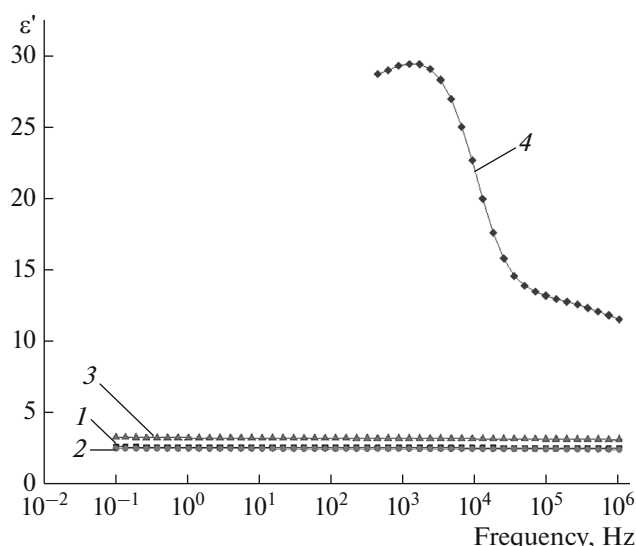


**Fig. 1.** Dependence of dielectric constant  $\epsilon'$  composites on frequency  $f$  at GNP concentrations of 0.1 (1), 0.25 (2), 1 (3), and 5 wt % (4).

tion of microcapacitors between adjacent filler particles, as a result of which the dielectric constant increases significantly and its dependence on frequency appears. As can be seen from the data in Fig. 2, at filler concentrations of  $>1$  wt %, the dependence of conductivity on frequency is linear in logarithmic coordinates, and at a filler concentration of 5 wt %, the conductivity reaches a plateau. The complete frequency dependence of conductivity has two compo-

nents: in a constant ( $\sigma_{dc}$ ) and frequency-dependent ( $\sigma_{ac}$ ) current. The horizontal section on the curve ( $dc$  conductivity) indicates that charge transfer occurs along an infinite cluster of contacting filler particles; i.e., at the given concentration, the percolation threshold is exceeded. The linear dependence on frequency ( $ac$  conductivity) indicates hopping conductivity between isolated filler particles, i.e., the concentration below the percolation threshold. In general, the dependence is described by the following equation:

$$\sigma(f) = \sigma_{dc} + \sigma_{ac} = \sigma_{dc} + Af^s,$$

where  $f$  is the frequency, and  $s$  is the parameter characterizing the features of hopping conduction [18]. We note the presence of two plateau areas for the sample with a filler concentration of 5 wt %, which may indicate the presence of two modes of charge transfer in this system. The high-frequency plateau (24700 Hz) corresponds to the transfer of charges in relatively large areas (aggregates of filler particles), and the low-frequency plateau (435 Hz) corresponds to the formation of contacts between these areas or aggregates and the movement of charges in the percolation cluster. The frequency at which the plateau is reached corresponds to the maximum in the frequency dependencies of the imaginary part of the electrical modulus  $M''$  (Fig. 3). Accordingly, the scales of the first and second regions differ by a factor of approximately 60. The sharp and significant increase in the dielectric constant (Fig. 2) also indicates that, at a filler concentration of 5 wt %, the percolation threshold has been exceeded.

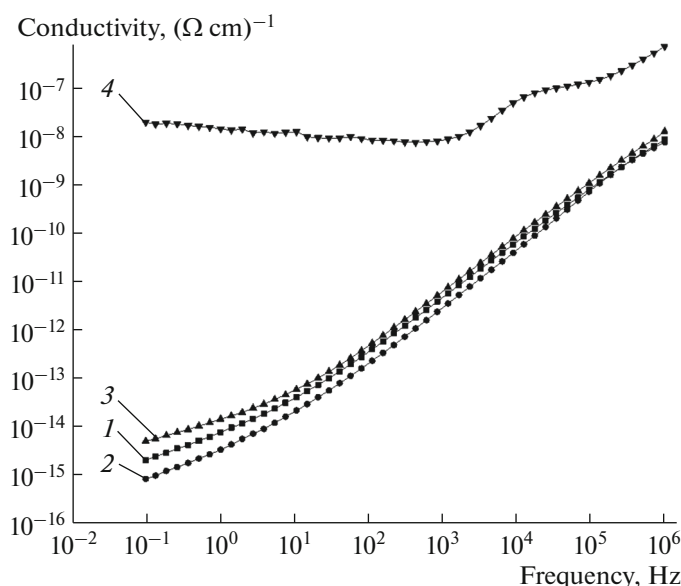


**Fig. 2.** Dependence of conductivity  $\sigma_{ac}$  of composites on frequency  $f$  at GNP concentrations of 0.1 (1), 0.25 (2), 1 (3), and 5 wt % (4).

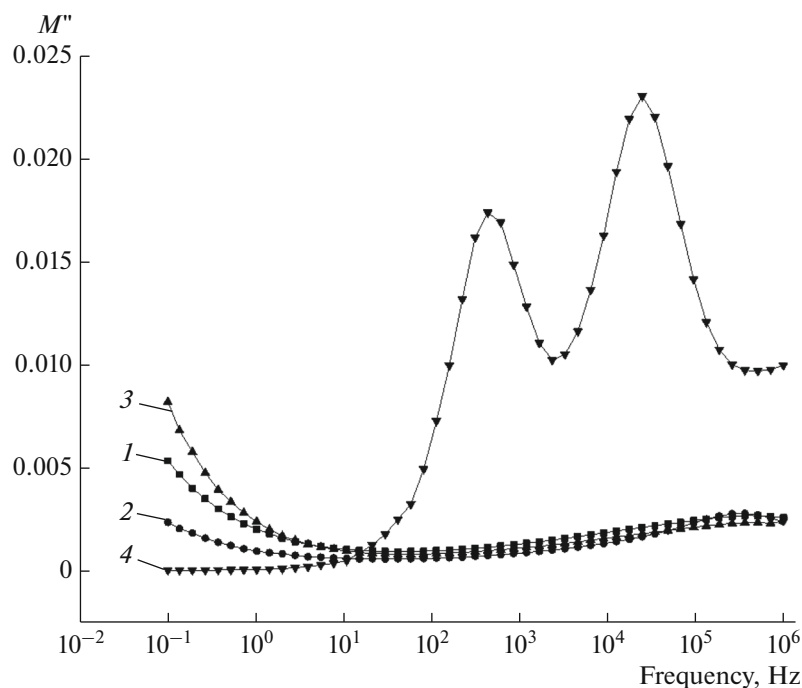


**Fig. 3.** Dependence of frequency  $f$  of imaginary part of the electrical module  $M''$  at GNP concentrations of 0.1 (1), 0.25 (2), 1 (3), and 5 wt % (4).

It is well known that the mechanical characteristics of composite materials are largely determined by the porosity of the structure. In relation to this, the porosity of PLA samples and PLA–GNP composites of various compositions before and after UV irradiation for 3 h was determined using X-ray microtomography. The results obtained are presented in Table 1.

**Table 1.** Porosity of original PLA and PLA–GNP composites before and after UV irradiation

GNP content in the composite, wt %	Porosity, vol %
Original composites	
PLA	5.9
0.1	7.3
0.25	7.4
1.0	7.2
5.0	14.5
Composites after UV irradiation (3 h)	
PLA	11.6
0.1	11.9
0.25	13.7
1.0	9.0
5.0	15.0

As can be seen from the data presented, the introduction of GNPs in the initial composites helps to increase the porosity of the samples, which practically remains unchanged in the range of filler concentrations of 0.1–1 wt %; however, an increase in its content to 5 wt % leads to the number of pores almost doubling.

At the same time, exposure to UV irradiation contributes to an increase in the number of pores, which is explained by the violation of the integrity of the material under these conditions. It should be noted that this process occurs most noticeably at low filler concentrations, while at higher concentrations (5 wt %), the observed effect is leveled out (the number of pores is 14.5 and 15.0, respectively). Apparently, in this case, the number of GNPs is sufficient to preserve the material from the destructive effects of UV irradiation.

The mechanical characteristics of PLA and its composites with GNPs are given in Table 2.

A comparative analysis of the data shows that an increase in the GNP content leads to a slight increase in the elastic modulus ( $E$ ) and a slight decrease in the tensile strength ( $\sigma_R$ ) and elongation at break ( $\epsilon_p$ ) values. We previously obtained similar results when studying the effect of rGO on the mechanical characteristics of PLA–rGO composites obtained by the solid-phase method [19]. In the general case, this type of change in mechanical characteristics is related to the influence of hard graphite-based nanofiller particles.

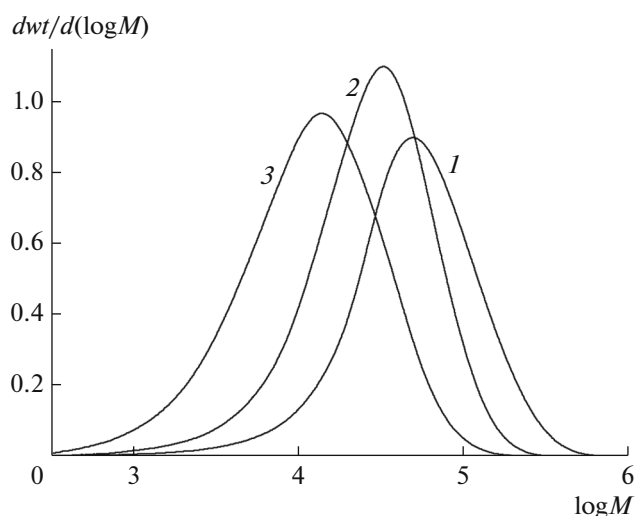
**Table 2.** Mechanical characteristics of the original PLA and PLA–GNP composites

GNP content in the composite, wt %	$E$ , MPa	$\sigma_p$ , MPa	$\epsilon_p$ , %
PLA	2700	45.4	4
0.05	2960	44.4	3
0.1	3155	46.9	3
0.15	3020	45.5	3
0.2	3170	40.9	3
0.25	3200	44.5	2
1	3220	40.7	2
5	3550	32.6	1

As already mentioned, during operation, products made of polymer composite materials may be exposed to UV radiation, which negatively affects their properties. In relation to this, the processes occurring in PLA–GNP composites during irradiation were studied by GPC, which makes it possible to evaluate the change in the molecular weight and molecular weight distribution (MWD) of PLA with irradiation time and by measuring the mechanical characteristics of the irradiated samples.

The molecular weight characteristics of the original PLA and in PLA–GNP composites of various compositions after exposure to UV radiation, depending on the irradiation time, are presented in Figs. 4 and 5 and in Table 3.

Figure 4 shows the MWD curves of the original PLA (curve 1) and PLA subjected to UV irradiation for 3 (curve 2) and 24 h (curve 3), plotted in semilogarithmic coordinates.

**Fig. 4.** MWD curves of PLA depending on the time of UV irradiation (1), 0; (2), 3; (3), 24 h.

As can be seen from the figure, in all MWD curves, there is only one peak; however, during irradiation, a shift in the maximum of the distribution curves is observed, indicating a decrease in the molecular weight of the samples (see Table 3).

Figure 5 shows the MWD curves of PLA-based composites containing from 0.1 to 5 wt % GNP, depending on the time of UV irradiation. It follows from the figure that during irradiation the MWD curves shift, which is especially noticeable after 24 h of irradiation. Although for composites containing 0.1 and 0.25 wt % GNP, there is no significant change in the MWD (Figs. 5b, 5c, curves 2, 3), for samples containing 1 and 5 wt % of the filler, the curves shift to the high-molecular region, which indicates the stabilizing effect of graphene fillers on the destruction of PLA under exposure to UV irradiation. In this case, the character of the distribution curves does not change; i.e., sequential destruction of the polymer chain occurs along the ester bonds [16], leading to a decrease in molecular weight and, as shown below, loss of mechanical stability of the samples.

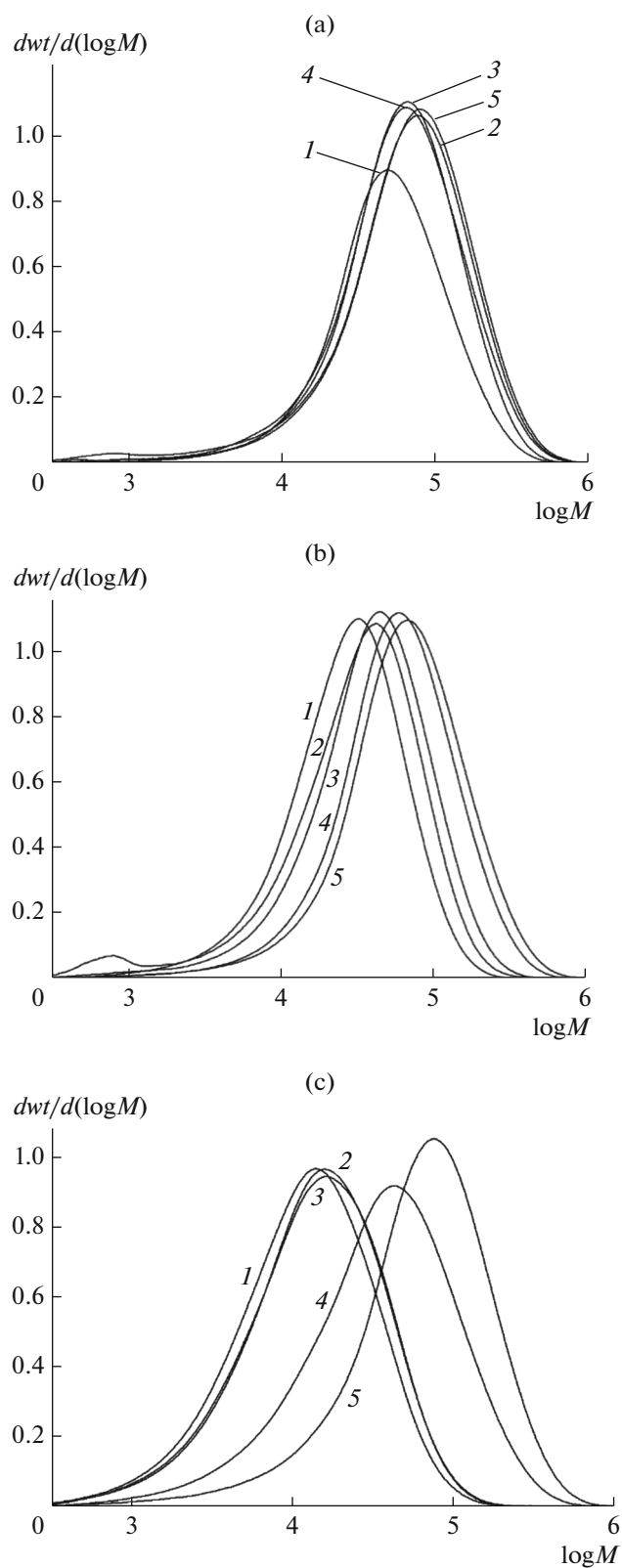
The results of measuring the MWD of PLA and PLA in composites of various compositions are presented in Table 3. From a comparative analysis of the data presented in the table, it follows that the change in the molecular weight of the samples depends on both the filler content and the time of UV irradiation. Although the  $M_w$  of PLA in a composite containing 1 wt % GNP after 3 h of irradiation is 80900, after 24 h of irradiation this value is only 57000. At the same time, for a composite with 5 wt % GNP molecular weight of PLA is 94160 and 92260, respectively; i.e., an increase in the GNP content has a stabilizing effect on the process of polyester destruction.

The results above are clearly illustrated by the curves shown in Fig. 6, demonstrating the influence of the nanofiller content on the change in the molecular weight (sample stability) of PLA in composites based on it.

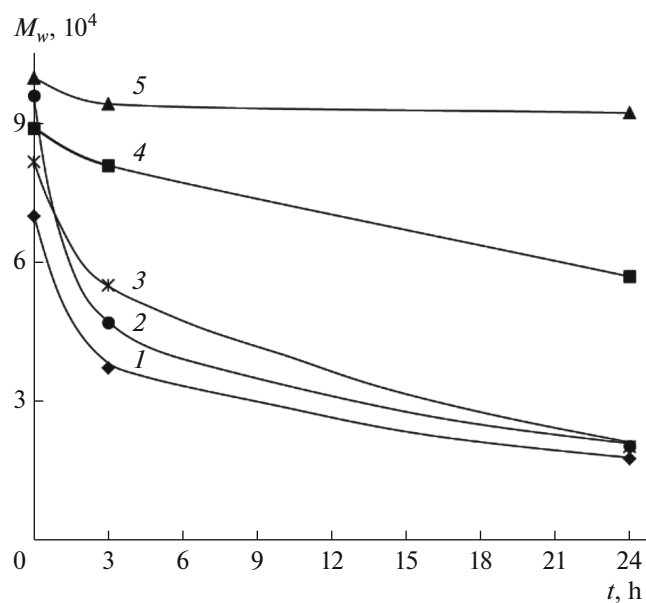
Since a decrease in the molecular weight of PLA during irradiation must inevitably affect its mechanical properties, a comparative study of changes in the mechanical characteristics of PLA and PLA–GNP composites of various compositions during irradiation was carried out in this paper.

Figure 7 shows the dependence of the mechanical characteristics of composites with different filler contents exposed to UV radiation on time.

As can be seen from the figure, UV irradiation leads to a sharp decrease in the values of all mechanical characteristics of composites with a low content of GNPs (0.1 wt %), which lose mechanical stability after 3 h of irradiation. At the same time, composites containing 0.25 wt % filler are destroyed only after 9 h of irradiation. Subsequent UV irradiation leads to the complete destruction of the films, and the onset of the destruction time increases with the increasing filler content.



**Fig. 5.** (a) MWD curves of composites based on PLA (1), containing 0.1 (2), 0.25 (3), 1 (4), and 5 wt % (5) GNP without exposure to UV irradiation; (b) MWD curves of composites based on PLA (1), containing 0.1 (2), 0.25 (3), 1 (4), and 5 wt % (5) GNP for 3 h. UV irradiation, (c) MWD curves of composites based on PLA (1), containing 0.1 (2), 0.25 (3), 1 (4), and 5 wt % (5) GNP for 24 h. of UV irradiation.



**Fig. 6.** Effect of UV irradiation time on  $M_w$  of initial PLA (1) and PLA in composites with GNPs of various compositions. Contents of the GNPs: 0.1 (2), 0.25 (3), 1.0 (4), 5 wt % (5).

**Table 3.** Molecular weight characteristics of the original PLA and in PLA–GNP composites depending on the time of UV irradiation

GNP content in composites, wt %	$M_n$	$M_w$	$M_p$	PD
0 h				
PLA	27800	70000	49400	2.5
0.10	34280	95940	77600	5.1
0.25	29730	81600	66370	3.4
1	29680	88930	65370	3.0
5	30060	99700	79940	3.3
3 h				
PLA	15570	37330	32780	2.4
0.10	19930	47060	42900	4.2
0.25	18120	55000	45240	3.0
1	30900	80900	60200	2.6
5	31750	94160	68630	3.0
24 h				
PLA	6320	17700	13740	2.8
0.10	7120	20460	15740	2.9
0.25	7100	20300	16000	2.9
1	15400	57000	42250	3.7
5	26470	92260	75250	3.5

$M_n$ , number average molecular weight;  $M_w$ , weight average molecular weight;  $M_p$ , molecular weight corresponding to the maximum of the chromatographic peak; PD, polydispersity.

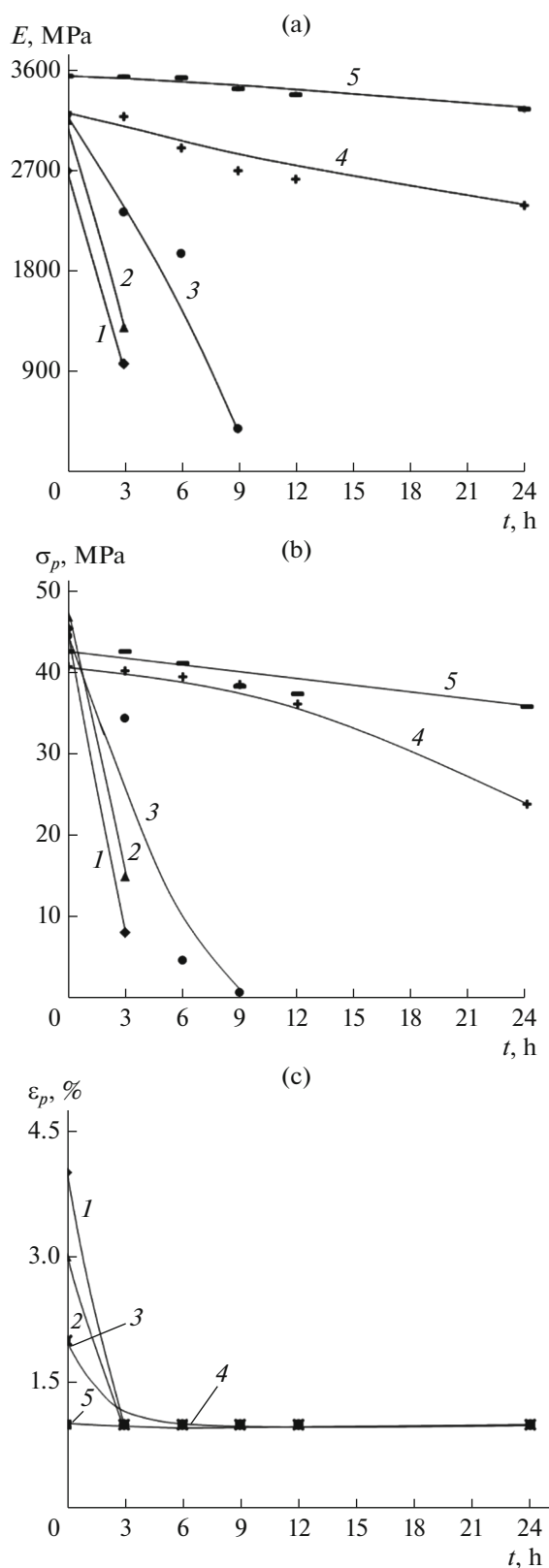


**Fig. 7.** (a) Dependence of elastic modulus  $E$  of composites of the original PLA (1) and PLA–GNP composites (0.1 (2), 0.25 (3), 1 (4), 5 wt % GNP (5)) on the time of UV irradiation; (b) dependence of elongation at break  $\sigma_R$  of composites of the original PLA (1) and PLA–GNP composites (0.1 (2), 0.25 (3), 1 (4), 5 wt % GNP (5)) on the time of UV irradiation; (c) dependence of elongation at break  $\epsilon_R$  of composites of the original PLA (1) and PLA–GNP composites (0.1 (2), 0.25 (3), 1 (4), 5 wt % GNP (5)) on the time of UV irradiation.



However, even at a GNP content of 1 and 5 wt %, only a slight decrease in the mechanical characteristics of the compositions is observed, which remain stable even after 24 h of UV irradiation. Apparently, this is due to the fact that at such concentrations, graphene nanoparticles have a sufficiently protective effect of PLA macromolecules from the destructive effects of UV irradiation, the rupture of polymer chains, which we described earlier in [16] when studying irradiated PLA using the IR spectroscopy method.

Thus, the data obtained convincingly demonstrate that the presence of GNPs increases the resistance of PLA-based composite films to UV radiation.

#### 4. CONCLUSIONS

Using the method of solid-phase mixing under the influence of shear deformations in a Brabender mixer, compositions of polylactide with graphite nanoparticles were obtained in a wide range of component ratios. The dependence of the electrical and mechanical properties of the materials being developed on their composition has been demonstrated.

A study of the electrical properties of the composites showed that the direct current conductivity of the composites appears at a filler concentration of 5 wt %; i.e., the percolation threshold lies in the range of 1–5 wt %. In a sample with a filler concentration of 5 wt %, a double percolation transition related to the aggregation of filler particles was detected.

During operation, polymer products can be exposed to aggressive environmental actions, in particular UV radiation, under the influence of which the destruction of polymer chains occurs, leading to a decrease in the molecular weight of the polymers and, as a consequence, loss of mechanical stability for products based on them.

Using X-ray microtomography, the porosity of the original samples and samples subjected to UV irradiation was determined, and their influence on the change in the mechanical characteristics of the composites was established.

In general, the introduction of nanofillers leads to an increase in the elastic modulus, as well as a decrease in the ultimate strength and elongation at break.

An effective method for assessing the impact of UV radiation on the characteristics of polymer products is to study them using exclusion chromatography, which allows evaluating changes in the molecular weight and molecular weight distribution. Based on the studies conducted, it was found that depending on the irradiation time (3 and 24 h), the maximum in the MWD curves shifts and the molecular weight of PLA decreases. The maximum drop in molecular weight was observed for composites with a low GNP content, while an increase in the content of nanofillers leads to an increase in their stability. A consequence of the decrease in the molecular weight of PLA is a decrease

in the mechanical characteristics of composites based on it, whose magnitude depends on both the content of the nanofillers and the irradiation time. In general, the composites with the maximum content of GNPs turned out to be the most resistant to UV irradiation, and their stability varied slightly depending on the irradiation time.

The results obtained make it possible to purposefully influence the properties of the resulting composites based on PLA and GNPs and contribute to the production of polymer materials that are resistant to UV irradiation.

#### FUNDING

This study was supported by the Russian Science Foundation (project no. 22-23-00369).

#### CONFLICT OF INTEREST

The authors of this work declare that they have no conflicts of interest.

#### REFERENCES

1. B. W. Chieng, N. A. Ibrahim, W. M. Z. W. Yunus, et al., *Polymer* **6**, 2232 (2014).  
<https://doi.org/10.3390/polym6082232>
2. D. G. Papageorgiou, I. A. Kinloch, and R. J. Young, *Prog. Mater. Sci.* **90**, 75 (2017).  
<https://doi.org/10.1016/j.pmatsci.2017.07.004>
3. K. J. Jem, J. F. van der Pol, and S. de Vos, *Microbial Lactic Acid, Its Polymer Poly(lactic acid) and their industrial Applications. Plastics from Bacteria: Natural Functions and Applications* (Royal Society of Chemistry, Gorinchem, The Netherlands, 2010).  
[https://doi.org/10.1007/978-3-642-03287-5\\_13](https://doi.org/10.1007/978-3-642-03287-5_13)
4. D. A. Garlotta, *J. Polym. Environ.* **19**, 63 (2001).  
<https://doi.org/10.1023/A:1020200822435>
5. A. Jiménez, M. Peltzer, and R. Ruseckaite, *Poly(lactic acid) Science and Technology Processing, Properties, Additives and Applications* (Royal Society of Chemistry, Cambridge, 2015).  
<https://doi.org/10.1039/9781782624806-FP005>
6. M. Zhang, X. Ding, Y. Zhan, Y. Wang, and X. Wang., *J. Hazard. Mater.* **384**, 121260 (2020).
7. B. Tawiah, Y. Bin, K. K. Y. Richard, et al., *Carbon* **150**, 8 (2019).  
<https://doi.org/10.1016/j.carbon.2019.05.002>
8. S. Z. Rogovina, M. M. Gasymov, S. M. Lomakin, O. P. Kuznetsova, et al., *Mech. Compos. Mater.* **58**, 845 (2023).  
<https://doi.org/10.1007/s11029-023-10073-2>
9. S. Z. Rogovina, S. M. Lomakin, S. V. Usachev, et al., *Polym. Cryst.* **2022**, 1 (2022).  
<https://doi.org/10.1155/2022/4367582>
10. T. Hideto, S. Hiroaki, S. Yoshihiro, *J. Polym. Environ.* **20**, 706 (2012).  
<https://doi.org/10.1007/s10924-012-0424-7>

11. T. S. Angelin, V. Ananthi, B. Abhispa, S. Nallathambi, et al., *Int. J. Biol. Macromol.* **234**, 123703 (2023).  
<https://doi.org/10.1016/j.ijbiomac.2023.123703>
12. E. Olewnik-Kruszkowska, I. Koter, J. Skopińska-Wiśniewska, et al., *J. Photochem. Photobiol. A. Chem.* **311**, 114 (2015).  
<https://doi.org/10.1016/j.jphotochem.2015.06.029>
13. R. S. Smykovskaya, O. P. Kuznetsova, T. I. Medintseva, et al., *Russ. J. Phys. Chem.* **41**, 1 (2022).
14. A. Sasov and D. Van Dyck, *J. Microsc.* **191**, 151 (1998).  
<https://doi.org/10.5772/32264>
15. T. I. Medintseva, A. I. Sergeev, N. G. Shilkina, et al., *Russ. J. Phys. Chem.* **42**, 61 (2023).  
<https://doi.org/10.31857/S0207401X23050096>
16. S. Z. Rogovina, S. M. Lomakin, S. V. Usachev, et al., *Appl. Sci.* **13**, 3920 (2023).  
<https://doi.org/10.3390/app13063920>
17. S. Z. Rogovina, E. V. Prut, K. V. Aleksanyan, et al., *J. Appl. Polym. Sci.* **136**, 47598 (2019).  
<https://doi.org/10.1002/app.47598>
18. A. K. Jonscher, *Nature* **267**, 673 (1977).  
<https://doi.org/10.1038/267673a0>
19. S. Z. Rogovina, S. M. Lomakin, M. M. Gasymov, et al., *Polym. Sci. Ser. D* **6**, 11 (2022).  
<https://doi.org/10.31044/1994-6260-2022-0-6-11-19>

**Publisher's Note.** Pleiades Publishing remains neutral with regard to jurisdictional claims in published maps and institutional affiliations.